



13TH CANADIAN MASONRY SYMPOSIUM
HALIFAX, CANADA
JUNE 4TH – JUNE 7TH 2017



**MODELLING OF THE CYCLIC RESPONSE OF AN UNREINFORCED MASONRY
WALL THROUGH A FORCE BASED BEAM ELEMENT**

Vanin, Francesco¹, Almeida, João² and Beyer, Katrin³

ABSTRACT

The seismic assessment of existing masonry buildings is based on the prediction of their nonlinear response under lateral loading. This requires a reliable estimation of the force and displacement demand. For this purpose, modelling strategies using structural component elements are widely applied both in research and in engineering practice, since they can provide a satisfactory description of the cyclic behaviour of a masonry building with a limited computational cost. One of such modelling strategies are equivalent frame models, in which beam elements describe the response of piers and spandrels.

This paper proposes the use of two-node, force-based beam elements with distributed inelasticity to model the in-plane response of modern unreinforced brick masonry panels. The nonlinearity of the response is described through the use of numerically integrated fibre sections and a suitable material model, implemented for this scope in the open-source platform “OpenSees”, describing a coupling at the local level between axial and shear response. Experimental results from a shear and compression test are used to validate the approach and justify some details of the proposed modelling strategy. Since the experimental data included also local displacement measures, the comparison of the numerical and experimental results is extended to curvatures and shear strains. The good agreement between numerical and experimental response confirms the applicability of the proposed approach for modelling the cyclic response of unreinforced brick masonry walls.

KEYWORDS: *force-based beam element, unreinforced masonry, cyclic in-plane behaviour, distributed inelasticity*

¹ PhD candidate, École Polytechnique Fédérale de Lausanne (EPFL), francesco.vanin@epfl.ch

² Post-doctoral researcher, École Polytechnique Fédérale de Lausanne (EPFL), joao.almeida@epfl.ch

³ Professor, École Polytechnique Fédérale de Lausanne (EPFL), katrin.beyer@epfl.ch

INTRODUCTION

The assessment of the seismic behaviour of masonry buildings through refined procedures, such as static non-linear analyses or incremental dynamic analyses, requires the use of accurate and efficient numerical tools for the prediction of the structural response, in terms of strength and displacement capacity, in the monotonic and, when needed, in the cyclic range. In this context, beam models, despite the strong kinematic assumptions that they imply, still represent typically a very good compromise between accuracy of the description of the cyclic response on one side, and simplicity and computational efficiency on the other side [1–3].

Beam models of masonry walls are meant to be applied to equivalent frame modelling approaches, in which the structure is simplified into a frame of deformable elements, corresponding to piers and, when present, spandrels, connected by rigid nodes. In equivalent frame models, damage is usually assumed to concentrate in the deformable beams or macro-elements, which have to give a complete description of the response of the structural element, including all the relevant non-linear phenomena and failure mechanisms that can affect it, such as the opening and closure of joints in flexure and the diagonal cracking of joints and, eventually, units in shear. Failure mechanisms are typically classified into flexural or rocking failure, and shear failure for diagonal cracking or, less often, for sliding in the joints [4]. However, in addition to these pure modes, mixed failure mechanisms are often observed in experimental tests [5].

Equivalent frame models for URM buildings make often use of macro-elements developed to reproduce the global force-displacement response of a masonry structural element. Although they provide information only at the global level, macro-elements owe their large diffusion to the numerical simplicity implied in the method. A well-known macro-element was proposed by Penna et al. [7].

A slightly more refined approach for the equivalent frame modelling of URM building is represented by beam models, in which global quantities such as nodal forces and displacements are computed together with local quantities (strains, stresses and sectional deformations). Among the beam element models with distributed plasticity, force-based formulations are often preferred over displacement-based elements because the force interpolation functions verify strictly equilibrium in each integration point.

Force-based beam models for modelling the response of URM walls were proposed by Roca [1] and more recently by Addessi et al. [9], resorting to simple non-linear elastic constitutive models through which the numerical integration throughout the sections can be avoided. As a more complex approach, applicable to the cyclic range, Raka et al. [10] recently proposed a force-based beam element with numerically integrated fibre sections for URM walls. The nonlinear behaviour in shear was tackled by a phenomenological cyclic law, uncoupled from the axial behaviour, describing the shear force-deformation relationship at the sectional level. Effects of the variable axial load on the shear capacity, and the influence of the partialisation of the section on the shear behaviour, are therefore not captured.

The present study proposes a force-based beam element for the modelling of URM walls that couples bending and shear behaviour. It is applicable to the cyclic range, opening up the possibility of conducting a large number of nonlinear time-history analyses with a limited numerical burden, which is one of the most appealing features of equivalent frame models. The axial and shear behaviour is coupled at the fibre level by means of a simple biaxial mechanical model, which is based on a Mohr-Coulomb type law. This model has been implemented by the authors in the software OpenSees [12] and will be available as a free tool for the research and professional community.

This paper presents the central idea of the formulation of the material model, and compares numerical and experimental results of a wall failing in shear. The adequacy of a beam structural model to describe the kinematics of a shear-dominated masonry wall is discussed through the comparison with experimentally obtained local deformation measures.

FORMULATION OF THE BEAM ELEMENT

The assumption of a standard Timoshenko beam model for a masonry pier implies the acceptance of the kinematic hypotheses related to the beam theory, among which the strongest and more questionable for squat masonry elements are the adoption of a continuum material model, a constant distribution of shear strains on the section and the planarity of the section in the deformed configuration. For what concerns shear deformations, after the onset of diagonal cracking in a shear wall, a non-uniform shear strain distribution is typically observed [13]. However, it is not possible to model the true nonlinearity of the shear deformation in the framework of the Timoshenko beam theory. Although alternative structural theories (higher order beam theories) can relax the latter condition assuming different deformation modes for the deformed section, in this study the classical Timoshenko beam theory is applied.

If one adopts a material model that assumes that only the compressed portion of the section contributes to its shear capacity—such as the model proposed by Roca [1]— the nonlinearity in the shear response is partially captured. The shear deformations remain, however, constant along the cross section and are therefore accounted for only in an average sense. However, the use of suitable material models can provide a rather refined description of the global behaviour of the element, despite the approximation that is made on local strains.

The use of a force-based beam element is suggested by the highly nonlinear profiles of sectional strains (i.e. curvatures and shear deformations) along the height of a masonry wall, that are observed in experimental tests. These profiles show the development of a region where non-linear deformations concentrate, that can be efficiently simulated by force-based beam elements, which do not make any assumption on the linearity of such deformation profiles.

The standard formulation of the Timoshenko force-based beam element as already implemented in OpenSees [12] is adopted. Fig. 1 shows some fundamental properties of the formulation. Shape functions are used to calculate sectional forces from the nodal forces, ensuring in this way strict

equilibrium at each integration section. The plane section hypothesis is used to calculate the strains (both normal and tangential components) at the fibre. A nonlinear bi-dimensional material model can then link these deformations to the stresses, accounting for their interaction.

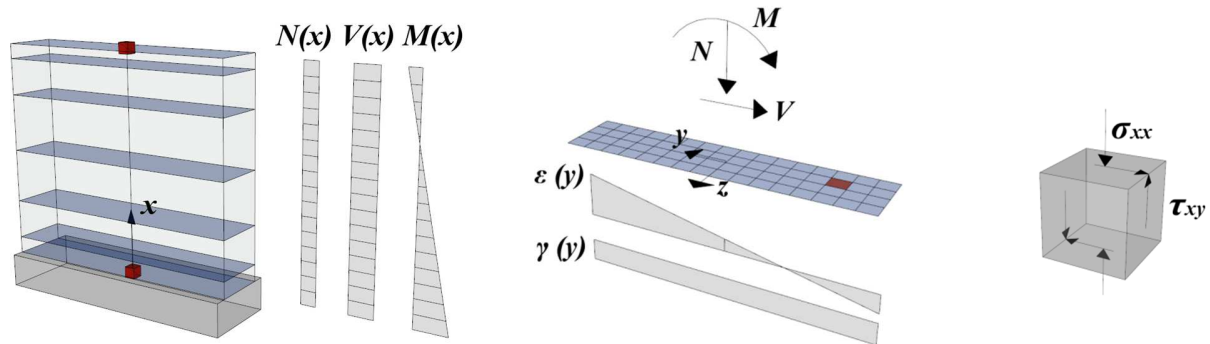


Fig. 1 – Formulation of the force-based beam element with coupling between axial and shear stress

Once the stress-strain response at the fibre level is established, numerical integration is performed along the section, and an iterative element-section state determination cycle has to be performed at each load step, rendering the solution of a force-based element less direct in comparison with a standard displacement-based element.

Material model

The nonlinear response of the element originates from the nonlinearity of the material model. As a minimum requirement, the used material model has to be formulated in a two-component strain/stress vector, including normal and tangential stresses. In order to be able to model all nonlinear phenomena that characterise the response of in-plane loaded masonry walls, the material model should describe complex nonlinear phenomena, such as:

- Crack opening in tension, and crack closure for reversed loading with stiffness recovery in compression, to properly model the rocking behaviour;
- Compressive failure to model toe crushing, with residual strains after damage in compression;
- Shear failure through a criterion able to take into account the influence of the axial load variation and of the decompression of part of the section under bending;
- Resistance to sliding along closed cracks, in cyclic rocking. This feature is complex to model with isotropic models that describe damage with scalar quantities independently of the direction, as the shear frictional strength would be improperly coupled with the tensile strength.

Considering these requirements, a simple constitutive model coupling axial and shear response was formulated and implemented in OpenSees. Fig. 2 represents the strength domain of the material model. The coupling between axial and shear stresses is ensured by the use of a Mohr-Coulomb (MC) type criterion, imposing a limit to the shear stress at each fibre depending on the current axial stress. Compressive failure is considered independent from the shear stresses, being the Mohr-Coulomb condition the only interaction between axial (σ) and shear (τ) stress components.

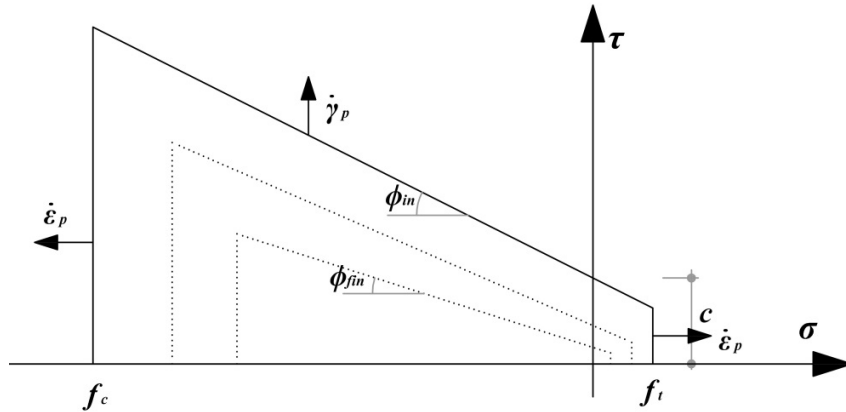


Fig. 2 – Yield domain of the material model

The basic steps in state determination of this simple biaxial material model are (1) the computation of the axial stress from the axial strain through a standard one-dimensional model, and (2) the computation of the shear stress based on the shear strain and on the updated value of axial stress, using a plastic model for shear. The material model adopted to describe the axial behaviour is the material Concrete 02, as already implemented in the source code of OpenSees. This model describes compressive damage and degradation of stiffness, hysteresis in the loading-reloading cycles, limited tensile strength, linear softening both in tension and compression, recovery of stiffness after crack closure, and a residual strength in compression.

The formulation of the plastic model for shear is based on a modification of the model proposed by Lourenço for interfaces [14], considering only the frictional criterion, formalised in the standard formulation of eq. 1 through the yield function f_{MC} . Zero dilatancy was accounted for. The cohesion c and the friction angle ϕ are expressed as function $\bar{\sigma}_{MC}$ of the hardening variable κ_{MC} , whose evolution is linked to the plastic multiplier λ and the rate of plastic strain $\dot{\gamma}_p$ through eq. 3. The adopted hardening/softening functions differ from the original model, featuring a parabolic hardening and a parabolic-exponential softening which depends on one material parameter, the fracture energy G_f^{II} for mode II fracture. The initial friction angle ϕ_{in} can degrade with evolution of the plastic strain maintaining a residual strength ϕ_{fin} . For each strain increment, an implicit return mapping scheme is applied.

$$f_{MC} = |\tau| + \sigma \tan \phi(\kappa_{MC}) - \bar{\sigma}_{MC}(\kappa_{MC}) \quad (1)$$

$$\tan \phi = \tan \phi_{in} + (\tan \phi_{fin} - \tan \phi_{in}) \frac{c - \bar{\sigma}_{MC}}{c} \quad (2)$$

$$\dot{\kappa}_{MC} = \dot{\lambda}, \quad \dot{\gamma}_p = \dot{\lambda} \frac{\tau_{trial}}{|\tau_{trial}|}, \quad \tau_{trial} = \tau_n + G \Delta \gamma_{n+1} \quad (3)$$

Since the cyclic behaviour of materials affected by cracking is poorly modelled by the classical theory of plasticity, several extensions have been proposed to properly account for inelastic phenomena during unloading and reloading cycles. The approach followed here is similar to the one adopted by Oliveira et al. [15], making use of auxiliary unloading surfaces that govern the variation of plastic strains. The evolution of such surfaces is governed by hardening laws that can reproduce a complex behavior of the material, as long as they respect few mathematical constraints, discussed in detail in Oliveira [16]. In this context, a simple linear evolution law was applied, modelling a loss of shear stiffness after the development of large inelastic strains, similarly to the model proposed by Aref and Dolatshahi [17]. An example of the resulting cyclic behaviour at the local scale is shown in Fig. 3 for the axial and shear components.

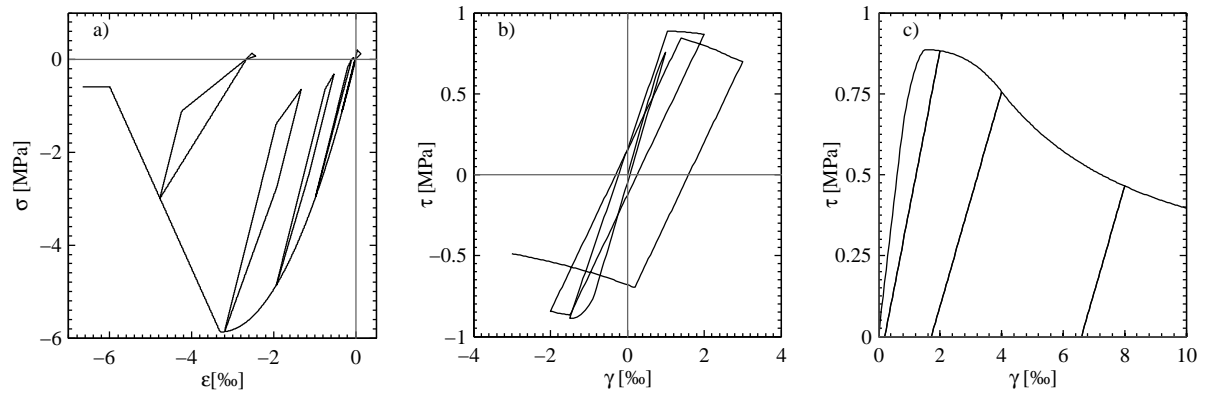


Fig. 3 – Cyclic behaviour of the material model in compression (a) and shear, under a constant axial load (b, c). Main material properties: $f_c = 5.7$ MPa, $f_t = 0.25$ MPa, $c = 0.25$ MPa, $\tan \phi_{in} = 0.4$, $\tan \phi_{fin} = 0.2$, $G_f^c = 8$ N/mm, $G_f^l = 0.05$ N/mm, $G_f^{ll} = 0.5$ N/mm

COMPARISON WITH EXPERIMENTAL RESULTS

The performance of the proposed beam element was compared to a quasi-static cyclic test on one URM wall, which was performed at EPFL. The wall was built with hollow clay brick units and standard cement-based mortar. The whole test campaign consisted of six quasi-static cyclic tests on identical walls, tested under different axial load ratios and moment restraints applied at the top of the walls. The test setup, shown in Fig. 4, comprised three servo-hydraulic actuators that could be controlled in a fully-coupled mode. The two vertical actuators allowed applying an axial force and moment at the top of the wall simulating several top boundary conditions that are different from the standard cantilever and fixed-fixed configurations typically applied in shear and compression wall tests.

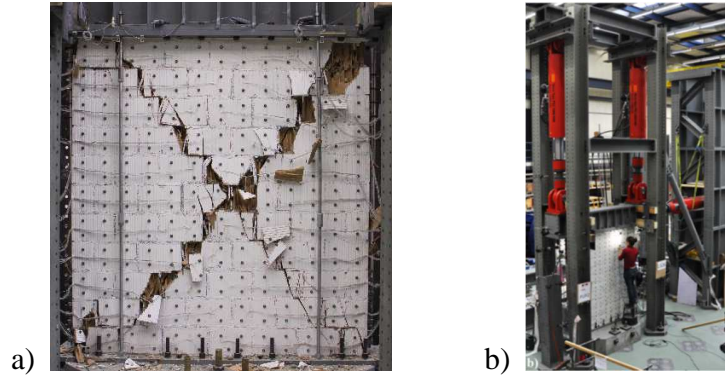


Fig. 4 –Wall PUP1 at failure (a), and test setup, showing the position of the three red actuators (b) [18]

Throughout the loading, the deformation of the walls was recorded through a digital photogrammetric measurement system, tracking the 3D position of 312 light emitting diodes (LEDs) for each test unit. The measurement of the LEDs' position at a frequency of 2 Hz allowed calculating the strain fields in the wall throughout the experiment. The whole dataset is publically available online [18].

Among the six tests, wall PUP1, which was modelled through the presented approach, exhibited a clear shear failure mode, with the development of two diagonal cracks. The dimensions of the wall are 2.25 m in height, 2.01 m in length and 0.20 m in thickness. A constant load of 419 kN was applied at the top of the wall, corresponding to an axial load ratio of 0.18. A moment was applied at the top section through the two vertical actuators, keeping a constant shear span of 0.5H, where H is the wall height. The main mechanical parameters derived from material tests on masonry wallets (compressive strength and elastic modulus) or calibrated for the numerical model are reported in Table 1.

Table 1 – Mechanical parameters, measured in the characterisation tests or calibrated for the numerical model

measured		calibrated			
f_c	5.87 MPa	G_f^I	0.05 N/m	c	0.20 MPa
E	3550 MPa	G_f^{II}	0.30 N/m	$\tan \phi_{in,}$	0.40
f_t	0.25 MPa	G_f^c	8 N/m	$\tan \phi_{fin,}$	0.13

Fig. 5 shows the comparison between the experimental global response of the wall and the numerical results, in terms of lateral force-displacement response. The Mohr-Coulomb criterion used at the material level controls the force capacity of the wall. The displacement capacity is governed by the fracture energy in mode II, which defines the post-peak behaviour of the material in shear. The accumulation of damage, and the consequent loss of lateral strength, after repeated

cycles, is captured by the model. However, as the post peak behaviour is rather sensitive to the choice of the fracture energy in shear, which is affected by a large uncertainty and seldom measured in experimental campaigns.

The energy dissipation depends on the model for the degradation of the shear stiffness after large plastic deformations. Classical plasticity models, with no evolution of plastic strains during unloading, lead to an overestimation of the energy dissipation of the wall. On the contrary, if a reduced stiffness is accounted for, an improved modelling of the cyclic response of the wall is obtained. In Fig. 5, a linear reduction of stiffness up to 30% of the initial stiffness at a plastic strain of 1% was calibrated to improve the match the with experimental results in the unloading branches.

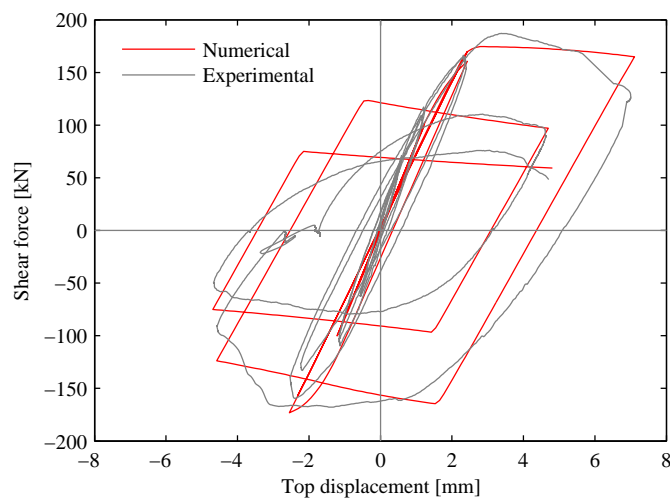


Fig. 5 – Comparison between experimental results and numerical force-displacement response of the beam element

The experimental displacement and strain fields, calculated from the LEDs measurements and presented in Fig. 6a-b, confirm that shear dominated walls present deformation modes that are not captured well by classical beam theories, which postulate that plane sections remain plane after deformation. Fig. 6c shows the amplified displacement field measured for the wall PUP1 at 0.15% drift, after the onset of diagonal cracking. A warping deformation due to shear, together with the opening of the diagonal crack, can be observed. While the latter cannot be described directly by beam models, the warping of the section could be captured by higher order beam theories. As mentioned, however, the warping deformation mode implies the use of an additional degree of freedom at the nodes, and the introduction at the sectional level of two generalised forces and deformations (a warping moment and a warping shear).

The deformation fields calculated for axial and shear strains are largely affected by the development of diagonal cracking, which renders the definition of the sectional strains more complex, and less objective, compared to the case of flexure dominated walls. If the strain profile along horizontal sections is approximated by a linear fit, however, curvatures and shear

deformations can be computed for each section. The comparison between the numerical predictions and the experimental measures is shown in Fig. 6d for 0.15% drift. The order of magnitude and the profile of shear strains agrees on average with the experimental measure. However, in the numerical model, the deformation in the post peak localises as expected in only one section, which is here the base section. For such shear dominated walls, therefore, both for the approximations introduced by the structural model and for numerical reasons, the comparison of local deformations is less accurate than it is in the case of flexural walls. However, despite the reduced accuracy of the modelling of the sectional response, the overall behavior of the wall could be captured.

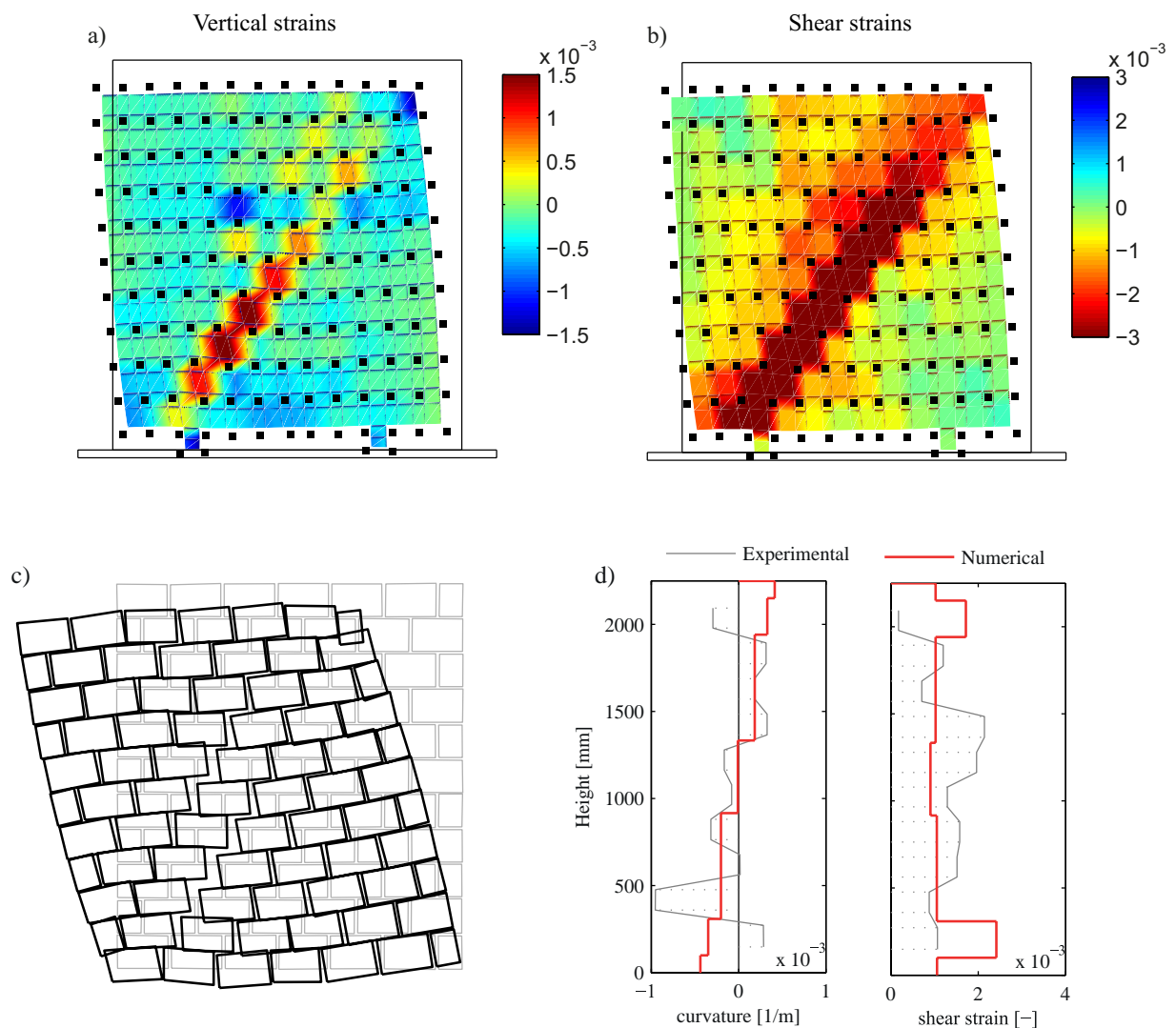


Fig. 6 – Local experimental deformation fields: vertical strains, (a) and shear strains (b). Deformed displacement field with warping of the sections due to shear (c). Comparison of experimental and numerical curvature and sectional shear deformation profiles (d)

CONCLUSIONS

Shear dominated walls exhibit a complex deformation field, characterized by a non-planar deformation of the sections and inelastic phenomena, such as diagonal cracking, that influence the response of the element. However, curvatures and sectional shear strains can be derived from linearization of the experimental strains, and show a nonlinear profile that can be modelled effectively by a single force-based beam element. Coupling the axial and shear response at the fibre level through 2D constitutive relationships can model directly the interaction between shear and decompression of the sections, and is able to reproduce with sufficient accuracy the experimental average deformation profiles of URM walls, as well as the global response of the element.

An improved plasticity based model able to capture the interaction of shear and axial stresses, and to describe both the loss of strength and the reduction of shear stiffness after large deformation has been implemented in OpenSees. When used in combination with a force-based element it provides a satisfactory modelling of the cyclic response of a shear dominated URM wall. If material models that include softening are used, localisation issues affect strongly the response in the post-peak branch. The choice of suitable material parameters defining the post peak (fracture energy in mode II) and the cyclic behavior (loss of stiffness), governs the modelling of the deformation capacity and the loss of strength for accumulation of damage.

Further research is needed to improve the modelling of the cyclic behavior of the implemented material model in shear, through more complex evolution laws that can capture better the characteristics of the cyclic response of a shear URM wall. Furthermore, the application of refined structural models, such as higher order beam theories modelling the warping of the beam section, can be investigated, as they could significantly improve, although at the cost of a higher numerical burden, the description of the experimentally observed displacement fields.

ACKNOWLEDGEMENTS

This project is supported by the Swiss Federal Office of the Environment and the Construction Department of the Canton Basel-Stadt.

REFERENCES

1. Roca P, Molins C, Marí AR. Strength Capacity of Masonry Wall Structures by the Equivalent Frame Method. *Journal of Structural Engineering* 2005; 131(10): 1601–1610. DOI: 10.1061/(ASCE)0733-9445(2005)131:10(1601).
2. Belmouden Y, Lestuzzi P. An equivalent frame model for seismic analysis of masonry and reinforced concrete buildings. *Construction and Building Materials* 2009; 23(1): 40–53. DOI: 10.1016/j.conbuildmat.2007.10.023.
3. Penna A, Senaldi I, Galasco A, Magenes G. Numerical Simulation Of Shaking Table Tests On Full-Scale Stone Masonry Buildings. *International Journal of Architectural Heritage* 2015; 3058. DOI: 10.1080/15583058.2015.1113338.
4. Magenes G, Calvi GM. In-plane seismic response of brick masonry walls. *Earthquake*

- Engineering Structural Dynamics* 1997; 26(11): 1091–1112. DOI: 10.1002/(SICI)1096-9845(199711)26:11<1091::AID-EQE693>3.0.CO;2-6.
5. Frumento S, Magenes G, Morandi P, Calvi GM. *Interpretation of experimental shear tests on clay brick masonry walls and evaluation of q-factors for seismic design*. Pavia (Italy): 2009.
 6. Lagomarsino S, Penna A, Galasco A, Cattari S. TREMURI program: An equivalent frame model for the nonlinear seismic analysis of masonry buildings. *Engineering Structures* 2013; 56: 1787–1799. DOI: 10.1016/j.engstruct.2013.08.002.
 7. Penna A, Lagomarsino S, Galasco A. A nonlinear macroelement model for the seismic analysis of masonry buildings. *Earthquake Engineering & Structural Dynamics* 2014. DOI: 10.1002/eqe.
 8. Gambarotta L, Lagomarsino S. Damage models for the seismic response of brick masonry shear walls. Part II: The continuum model and its applications. *Earthquake Engineering & Structural Dynamics* 1997; 26: 441–462. DOI: 10.1002/(sici)1096-9845(199704)26:4%3C441::aid-eqe651%3E3.0.co;2-0.
 9. Addessi D, Liberatore D, Masiani R. Force-Based Beam Finite Element (FE) for the Pushover Analysis of Masonry Buildings. *International Journal of Architectural Heritage* 2014; 9(3): 231–243. DOI: 10.1080/15583058.2013.768309.
 10. Raka E, Spacone E, Sepe V, Camata G. Advanced frame element for the seismic analysis of masonry structures: model formulation and validation. *Earthquake Engineering & Structural Dynamics* 2015. DOI: 10.1002/eqe.
 11. Ghiassi B, Soltani M, Tasnimi AA. A simplified model for analysis of unreinforced masonry shear walls under combined axial, shear and flexural loading. *Engineering Structures* 2012; 42: 396–409. DOI: 10.1016/j.engstruct.2012.05.002.
 12. McKenna F, Fenves GL, Scott MH, Jeremic B. Open System for Earthquake Engineering Simulation (OpenSees) 2000.
 13. Sinha BP, Maurenbrecher HP, Hendry AW. Model and Full-scale Tests on a Five-Storey Cross-wall Structure Under Lateral Loading. *2nd International Brick Masonry Conference*, Stoke-on-Trent, UK: 1971.
 14. Lourenço PB. *Computational strategies for masonry structures*. vol. 70. Delft University Press; 1996. DOI: ISBN 90-407-1221-2.
 15. Oliveira D V., Lourenço PB. Implementation and validation of a constitutive model for the cyclic behavior of interface elements. *Computers and Structures* 2004; 82.
 16. Oliveira DV. *Experimental and Numerical Analysis of Blocky Masonry Structures Under Cyclic Loading*. University of Minho, 2003.
 17. Aref AJ, Dolatshahi KM. A three-dimensional cyclic meso-scale numerical procedure for simulation of unreinforced masonry structures. *Computers and Structures* 2013; 120: 9–23. DOI: 10.1016/j.compstruc.2013.01.012.
 18. Petry S, Beyer K. Cyclic test data of six unreinforced masonry walls with different boundary conditions. *Earthquake Spectra* 2014; 31(4): 140916115854000. DOI: 10.1193/101513EQS269.

